

La³⁺-Catalyzed Methanolysis of *N*-Aryl- β -lactams and Nitrocefim

Pedro J. Montoya-Pelaez, Graham T. T. Gibson, Alexei A. Neverov, and R. S. Brown*

Department of Chemistry, Queen's University, Kingston, Ontario, Canada K7L 3N6

Received September 8, 2003

The kinetics of the La³⁺-catalyzed methanolysis of *N*-phenyl- β -lactam (**2**) and *N*-*p*-nitrophenyl- β -lactam (**3**) as well as that of nitrocefim (**1**) were studied at 25 °C under buffered conditions. In the case of **2** and **3**, the observed second-order rate constants (k_2^{obs}) for catalysis plateau at \sim pH 7.5–7.8, reaching values of 1×10^{-2} and $35 \times 10^{-2} \text{ M}^{-1} \text{ s}^{-1}$ respectively. Potentiometric titrations of solutions of $2 \times 10^{-3} \text{ M}$ La(OTf)₃ were analyzed in terms of a dimer model (La³⁺₂(-OCH₃)_{*n*}), where the number of methoxides varies from 1 to 5. The species responsible for catalysis in the pH range investigated contain 1–3 methoxides, the one having the highest catalytic activity being La³⁺₂(-OCH₃)₂, which comprises 80% of the total La³⁺ forms present at its pH maximum of 8.9. The catalysis afforded by the La³⁺ dimers at a neutral pH is impressive relative to the methoxide reactions: at pH 8.4 a 1 mM solution of catalyst (generated from 2 mM La(OTf)₃) accelerated the methanolysis of **2** by $\sim 2 \times 10^7$ -fold and **3** by $\sim 5 \times 10^5$ -fold. As a function of metal ion concentration, the La³⁺-catalyzed methanolysis of **1** proceeds by pathways involving first one bound metal ion and then a second La³⁺ leading to a plateau in the k_{obs} vs [La³⁺]_{total} plots at all pH values. The $k_{\text{max}}^{\text{obs}}$ pseudo-first-order rate constants at the plateaus, representing the spontaneous methanolysis of La³⁺₂(1⁻) forms, has a linear dependence on [-OCH₃] (slope = 0.84 ± 0.05 if all pH values are used and 1.02 ± 0.03 if all but the two highest pH values are used). The speciation of bound **1** at a La³⁺ concentrations corresponding to that of the onset of the kinetic plateau region was approximated through potentiometric titration of the nonreactive 3,5-dinitrobenzoic acid in the presence of 2 equiv of La(OTf)₃. A total speciation diagram for all bound forms of La³⁺₂(1⁻)(-OCH₃)_{*n*}, where *n* = 0–5, was constructed and used to determine their kinetic contributions to the overall pH vs $k_{\text{max}}^{\text{obs}}$ plot under kinetic conditions. Two kinetically equivalent mechanisms were analyzed: methoxide attack on La³⁺₂(1⁻)(-OCH₃)_{*n*}, *n* = 0–2; unimolecular decomposition of the forms La³⁺₂(1⁻)(-OCH₃)_{*n*}, *n* = 1–3.

Introduction

The β -lactam antibiotics are widely used to combat bacterial infections,¹ but resistance to these² through the evolution of β -lactamases presents a serious threat to human health. The mechanisms of action of the class A, C, and D serine-based β -lactamases are reasonably well understood.³ However, the class B Zn²⁺- β -lactamases⁴ have recently become both a major research area and clinical problem since these hydrolyze virtually all the β -lactam antibiotics including the broad-spectrum carbapenems and clavulanic acid. Several

members of the mononuclear⁵ and dinuclear⁶ Zn²⁺- β -lactamases are under active investigation, but a detailed picture of the mechanism, and particularly the role of the second

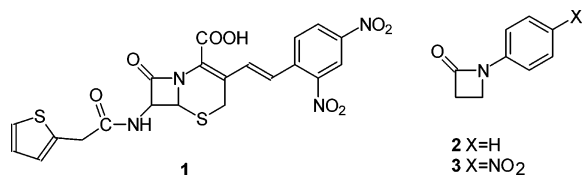
* To whom correspondence should be addressed. E-mail: Rsbrown@chem.queensu.ca.

- (1) (a) Neu, H. C. In *The Chemistry of β -Lactams*; Page, M. I., Ed.; Blackie: Glasgow, U.K., 1992; pp 192–128. (b) Page, M. I. *Adv. Phys. Org. Chem.* **1987**, 23, 165.
- (2) (a) Page, M. I. *Acc. Chem. Res.* **1984**, 17, 144. (b) Davies, J. *Science* **1994**, 264, 375. (c) Massova, I.; Mobashery, S. *Acc. Chem. Res.* **1997**, 30, 162.
- (3) Payne, D. J. *J. Med. Microbiol.* **1993**, 39, 93.

- (4) (a) Lipscomb, W. N.; Sträter, N. *Chem. Rev.* **1996**, 96, 2375 and references therein. (b) Cricco, J. A.; Orellano, E. G.; Rasia, R. M.; Ceccarelli, E. A.; Vila, A. J. *Coord. Chem. Rev.* **1999**, 190–192, 519. (c) Concha, N. O.; Janson, C. A.; Rowling, P.; Pearson, S.; Cheever, C. A.; Clarke, B. P.; Lewis, C.; Galleni, M.; Frère, J.-M.; Payne, D. J.; Bateson, J. H.; Abdel-Meguid, S. S. *Biochemistry* **2000**, 39, 4288. (d) Ullah, J. H.; Walsh, T. R.; Taylor, I. A.; Emery, D. C.; Verma, C. S.; Gamblin, S. J.; Spencer, J. *J. Mol. Biol.* **1998**, 284, 125. (e) Fabiane, S. M.; Sohi, M. K.; Wan, T.; Payne, D. J.; Bateson, J. H.; Mitchell, T.; Sutton, B. J. *Biochemistry* **1998**, 37, 12404. (f) Concha, N. O.; Rasmussen, B. A.; Bush, K.; Herzberg, O. *Structure* **1996**, 4, 823.
- (5) (a) Bicknell, R.; Schäffer, A.; Walley, S. G.; Auld, D. S. *Biochemistry* **1986**, 25, 7208. (b) Bounaga, S.; Laws, A. P.; Gallei, M.; Page, M. I. *Biochem. J.* **1998**, 331, 703. (c) Page, M. I.; Laws, A. P. *J. Chem. Soc., Chem. Commun.* **1998**, 1609.
- (6) (a) Wang, Z.; Fast, W.; Benkovic, S. J. *Biochemistry* **1999**, 38, 10013. (b) Fast, W.; Wang, Z.; Benkovic, S. J. *Biochemistry* **2001**, 40, 1640. (c) McManus-Munoz, S.; Crowder, M. W. *Biochemistry* **1999**, 38, 1547.

Zn²⁺, has yet to emerge. The mechanism of action of the mononuclear β-lactamase II from *Bacillus cereus*⁷ was proposed to involve the addition of a Zn²⁺-coordinated hydroxide to the β-lactam carbonyl.⁵ An available X-ray structure of the dinuclear enzyme from *B. fragilis* positions the two metals close enough together that they are bridged by a μ-hydroxy (or μ-aquo) group which is proposed to be the active nucleophile.^{4f} It has been suggested^{6a} that the two-metal ion mechanism is similar to that proposed for other dinuclear hydrolases⁸ with one metal ion providing the bound HO⁻ nucleophile while the other helps to (a) position the substrate for proper nucleophilic attack, (b) polarize further the (N)C=O scissile bond, and (c) stabilize the negative charge developed on the leaving group.

Earlier studies have reported the effects of divalent metal ions on the aqueous hydrolysis of benzyl penicillin^{9a-c} and cephaloridine.^{9c} The metal ion binds to the carboxylate of the penicillin or cephalosporin to facilitate an attack of external (or Zn²⁺-bound) hydroxide on the β-lactam C=O with possible facilitation of the breakdown of the tetrahedral intermediate through binding to the lactam N. β-Lactam degradation in methanol has been reported¹⁰ to be promoted by Cd²⁺ under non-pH-controlled conditions although a detailed mechanism for activity was not offered. A few simple mononuclear and dinuclear models for the Zn²⁺-β-lactamases were studied,¹¹ but the catalysis of hydrolysis of nitrocefin (**1**) was modest even though preequilibrium binding of the metal complex with the substrate was required. Moreover, a catalytic role for the second Zn²⁺ could not be established since mononuclear complexes seemed to be as effective as the dinuclear ones.



Our own work along these lines has described the Zn²⁺-catalyzed methanolysis of **1** and showed that pathways involving one and two Zn²⁺-ions were operative.¹² It was also reported in that study that Zn²⁺ did not catalyze the methanolysis of two simple lactams (**2**, **3**). Presently, we deal with La³⁺ catalysis of the methanolysis of **1** and lactams **2** and **3**. Although La³⁺ cannot be considered a biomimetic metal ion, we have shown in several reports that it promotes

the methanolysis of a variety of substrates¹³ including acetylimidazole,^{14a} activated and unactivated esters,^{14b} phosphate diesters,^{14c} (2-hydroxypropyl)-*p*-nitrophenyl phosphate,^{14d} and the phosphate triester paraoxon^{14e} through catalysis by a bis(μ-methoxy)-bridged La³⁺ dimer which is spontaneously formed in methanol. The dinuclear characteristics of that species structurally, at least, resembles the dinuclear core of a Zn²⁺-β-lactamase and prompted us to investigate whether it can facilitate the breakdown of lactams. Herein we show that the bis(μ-methoxy)-bridged La³⁺ dimer, formulated as La³⁺₂(-OCH₃)₂, imparts generous catalysis to the methanolysis of the two simple lactams and that the methanolysis of **1** is also promoted by La³⁺ through one- and, far more effectively, two-metal ion pathways.

Experimental Section

Materials. Nitrocefin (**1**) was purchased from Oxoid. Methanol (99.8% anhydrous), sodium methoxide (0.5 M), HClO₄ (70%, BDH), and acetonitrile (99.8% anhydrous) were all purchased from Aldrich and used without any further purification. 3,5-Dinitrobenzoic acid was purchased from Eastman Kodak and used as received. La(OTf)₃ was purchased from Aldrich and used as supplied. Lactams **2** and **3** were prepared according to published procedures.¹⁵

^spH Measurements.¹⁶ The CH₃OH₂⁺ concentration was determined using a Radiometer pHC4000-8 combination (glass/calomel) electrode for kinetic and titration measurements, calibrated with Fisher Certified Standard aqueous buffers (pH = 4.00 and 10.00), as described in our recent papers.^{13,14} Values of ^spH were calculated by subtracting a correction constant of -2.24 to the experimental meter reading (^wpH) as described by Bosch et al.¹⁷ The ^spK_a values of buffers used for the present kinetic studies were obtained from the literature¹⁷ or measured at half-neutralization of the bases with HClO₄ in MeOH.

^spK_a Determination. The potentiometric titrations of La(OTf)₃ and 3,5-dinitrobenzoic acid in methanol were performed using a Radiometer Vit 90 Autotitrator under anaerobic conditions (Ar) at 25.0 ± 0.1 °C. Methanolic La(OTf)₃ and 3,5-dinitrobenzoic acid stock solutions (0.25 M) were diluted to 0.01 or 0.02 and 0.01 M, respectively, the total sample volume being 20.0 mL. Sodium methoxide titrant, prepared from stock 0.5 M NaOCH₃ in a Sure Seal bottle, was 0.117 M and was calibrated by titrating Fisher Certified Standard HCl in water, with the end point taken to be

(7) Sabath, L. B.; Abraham, E. P. *Biochem. J.* **1966**, *98*, 11c.

(8) Wilcox, D. E. *Chem. Rev.* **1996**, *96*, 2435.

(9) (a) Cressman, W. A.; Sugita, E. T.; Doluisio, J. T.; Niebergall, P. J. *J. Pharm. Sci.* **1969**, *58*, 1471. (b) Gensmantel, N. P.; Gowling, E. W.; Page, M. I. *J. Chem. Soc., Perkin Trans. 2* **1978**, 335. (c) Gensmantel, N. P.; Proctor, P.; Page, M. I. *J. Chem. Soc., Perkin Trans. 2* **1980**, 1725.

(10) Martinez, J. H.; Navarro, P. G.; Garcia, A. A. M.; de las Parras, P. J. *M. Int. J. Biol. Macromol.* **1999**, *25*, 337.

(11) (a) Kaminskaia, N. V.; He, C.; Lippard, S. J. *Inorg. Chem.* **2000**, *39*, 3365. (b) Kaminskaia, N. V.; Spingler, B.; Lippard, S. J. *J. Am. Chem. Soc.* **2000**, *122*, 6411. (c) Kaminskaia, N.; Spingler, B.; Lippard, S. J. *J. Am. Chem. Soc.* **2001**, *123*, 6555.

(12) Montoya-Pelaez, P. J.; Brown, R. S. *Inorg. Chem.* **2002**, *41* 309–316.

(13) Brown, R. S.; Neverov, A. A. *J. Chem. Soc., Perkin Trans. 2* **2002**, 1039.

(14) (a) Neverov, A. A.; Brown, R. S. *Can. J. Chem.* **2000**, *78*, 1247. (b) Neverov, A. A.; McDonald, T.; Gibson, G.; Brown, R. S. *Can. J. Chem.* **2001**, *79*, 1704. (c) Neverov, A. A.; Brown, R. S. *Inorg. Chem.* **2001**, *40*, 3588. (d) Tsang, J.; Neverov, A. A.; Brown, R. S. *J. Am. Chem. Soc.* **2003**, *125*, 1559. (e) Tsang, J.; Neverov, A. A.; Brown, R. S. *J. Am. Chem. Soc.* **2003**, *125*, 7602.

(15) (a) Manhas, M.; Jeng, S. J. *Org. Chem.* **1967**, *32*, 1246. (b) Blackburn, G.; Plackett, J. J. *J. Chem. Soc., Perkin Trans. 2* **1972**, 1366.

(16) For the definitions of ^spH see the recommendations of the IUPAC: *Compendium of Analytical Nomenclature. Definitive Rules 1997*, 3rd ed.; Blackwell: Oxford, U.K., 1998. If one calibrates the measuring electrode with aqueous buffers and then measures the pH of an aqueous buffer solution, the term ^wpH is used, if the electrode is calibrated in water and the “pH” of the neat buffered methanol solution is measured, the term ^spH is used, and if the latter reading is made and the correction factor of 2.24 (in the case of methanol) is added, then the term ^spH is used.

(17) (a) Bosch, E.; Rived, F.; Roses, M.; Sales, J. *J. Chem. Soc., Perkin Trans. 2* **1999**, 1953. (b) Rived, F.; Roses, M.; Bosch, E. *Anal. Chim. Acta* **1998**, *374*, 309. (c) Bosch, E.; Bou, P.; Allemann, H.; Roses, M. *Anal. Chem.* **1996**, 3651.

$w\text{pH} = 7$. The standard titration protocol^{13,14} was adopted where after each titration the electrode was immersed in pH 4.00 aqueous buffer until the meter reading stabilized, a process that can take several minutes. The electrode was then rinsed with MeOH, dried with a tissue, and used for the next titration. The electrode was recalibrated often to ensure accurate readings.

The values of the species formation constants in methanol were calculated using the computer program Hyperquad 2000 (version 2.1 NT),¹⁸ with the autoprotolysis constant of pure methanol taken to be $10^{-16.77}$ at 25 °C.¹⁷ The formation constant for the species $\text{La}^{3+}_2(3,5\text{-dinitrobenzoate}^-)$, as a model for the species $\text{La}^{3+}_2(\mathbf{1})$, was calculated from the first 0.5 equiv of the titration of a 1:0.5 solution of $\text{La}(\text{OTf})_3$ -3,5-dinitrobenzoic acid (corresponding to deprotonation of the bound carboxylic acid) in comparison with the $s\text{p}K_a$ of the unbound acid obtained from simple titration in methanol. The formation constant for $\text{La}^{3+}(\mathbf{1}^-)$ was determined from titration of a 1:1 solution of $\text{La}(\text{OTf})_3$ -3,5-dinitrobenzoic acid by assessing the reduction in $s\text{p}K_a$ of the COOH functionality in the presence of metal ion. Formation constants for the $\text{La}^{3+}_2(\text{-OCH}_3)_n$ species were obtained from Hyperquad analysis of the titration of a 0.002 M solution of $\text{La}(\text{OTf})_3$ in methanol as reported.¹⁹ Because the metal-bound forms of $\mathbf{1}$ are too reactive to allow its titration in the presence of La^{3+} , the formation constants for all $\text{La}^{3+}_2(\mathbf{1}^-)(\text{-OCH}_3)_x$ species were assumed to be the same as those obtained from titration of 1:0.5 $\text{La}(\text{OTf})_3$ -3,5-dinitrobenzoic acid using all but the first 0.5 equiv, inputting all the $\text{La}^{3+}_2(\text{-OCH}_3)_n$ formation constants¹⁹ as known values in the program.

Kinetic Measurements. The rate of appearance of the methanolized product of $\mathbf{1}$ and $\mathbf{3}$ was followed by monitoring the increase in absorbance of buffered methanol solutions at 480 and 380 nm, respectively, with an OLIS-modified Cary 17 UV-Vis spectrophotometer or an Applied Photophysics SX-17MV stopped-flow reaction analyzer at 25.0 ± 0.1 °C. The rate of disappearance of $\mathbf{2}$ was followed by monitoring the decrease in absorbance of buffered methanol solutions at 250 nm with the OLIS-modified Cary spectrophotometer. All runs were repeated at least in duplicate. Reactions were monitored under pseudo-first-order conditions having a $[\text{La}^{3+}]$ ranging $(0.006\text{--}4.0) \times 10^{-3}$ M. Slow reactions, monitored using conventional UV analysis, were initiated by addition of an aliquot of a 2.0×10^{-3} M stock solution of $\mathbf{1}$ in CH_3CN (with 2.5% MeOH) to 2.5 mL of the buffered reaction mixture (final concentration of $\mathbf{1} = (0.8\text{--}2.0) \times 10^{-5}$ M). For $\mathbf{2}$ and $\mathbf{3}$, 10 μL of a 2.5×10^{-2} M stock solution in CH_3CN was added giving a final concentration of 5×10^{-5} M. For fast reactions of $\mathbf{1}$ monitored using the stopped-flow apparatus, one drive syringe was charged with $\mathbf{1}$ in 0.02 M buffer, while the second syringe contained twice the desired concentration of La^{3+} and 0.02 M buffer. The final concentration of β -lactam was in the range $(0.8\text{--}2.0) \times 10^{-5}$ M. Reactions were followed for at least 4 half-lives and displayed good first-order behavior. Pseudo-first-order rate constants (k_{obs}) for methanolysis were determined by NLLSQ fitting of the abs vs time traces to a standard exponential model. In the low $s\text{pH}$ runs for $\mathbf{2}$, due to the slow rate of the reaction, the low concentrations of metal were followed to $\sim 10\%$ completion and k_{obs} was determined using the initial rates method, with the ΔAbs value being determined from the faster runs where the reaction proceeded to completion. Buffering agents used were 2,6-lutidine ($s\text{p}K_a = 6.86$), *N*-methylimidazole ($s\text{p}K_a = 7.60$), *N*-ethylmorpholine ($s\text{p}K_a = 8.28$), and trimethylamine ($s\text{p}K_a = 9.80$ ^{17b}) partially neutralized with 70% HClO_4 , and the total buffer concentration

(18) Gans, P.; Sabatini, A.; Vacca, A. *Talanta* **1996**, *43*, 1739.

(19) Gibson, G.; Neverov, A. A.; Brown, R. S. *Can. J. Chem.* **2003**, *81*, 495.

Table 1. k_2^{obs} vs $s\text{pH}$ for $\text{La}(\text{OTf})_3$ -Catalyzed Methanolysis of β -Lactam $\mathbf{2}$ ($T = 25$ °C)

$s\text{pH}$	$10^3 k_2^a / \text{M}^{-1} \text{s}^{-1}$	$s\text{pH}$	$10^3 k_2^a / \text{M}^{-1} \text{s}^{-1}$
7.29	1.5 ± 0.2	8.09	8.8 ± 0.7
7.53	3.5 ± 0.2	8.30	9.3 ± 0.7
7.84	7.3 ± 0.4	8.72	10.1 ± 0.1
8.02	7.8 ± 0.4	8.92	10.7 ± 0.4

^a Error is taken as the standard error of the linear regression of the k_{obs} vs $[\text{La}^{3+}]_t$ data.

Table 2. k_2^{obs} vs $s\text{pH}$ for $\text{La}(\text{OTf})_3$ -Catalyzed Methanolysis of β -Lactam $\mathbf{3}$ ($T = 25$ °C)

$s\text{pH}$	$10^2 k_2^a / \text{M}^{-1} \text{s}^{-1}$	$s\text{pH}$	$10^2 k_2^a / \text{M}^{-1} \text{s}^{-1}$
7.03	3.2 ± 0.1	8.12	38.8 ± 1.1
7.34	6.5 ± 0.3	8.29	35.0 ± 0.6
7.42	13.6 ± 0.3	8.35	32.9 ± 1.6
7.56	14.5 ± 1.0	8.61	33.2 ± 0.7
7.81	21.5 ± 0.4	9.40	42.8 ± 2.5
8.02	29 ± 10	9.75	39.3 ± 2.3

^a Error is taken as the standard error of the linear regression of the k_{obs} vs $[\text{La}^{3+}]_t$ data.

was 2×10^{-2} M. There is always some small quantity ($< 0.1\%$) of water present stemming from that present in the MeOH and what is derived from buffer neutralization with 70% HClO_4 . To avoid any chloride ion contamination from the glass electrode that might affect the metal ion reactions, duplicate solutions were prepared, one for $s\text{pH}$ measurements and the second portion being used for kinetics. In all cases, $s\text{pH}$ values measured before and after reaction were consistent to within 0.05 units.

Results

Kinetics of La^{3+} -Catalyzed Methanolysis of β -Lactams

1–3. The pseudo-first-order rate constants for methanolysis of $\mathbf{2}$ and $\mathbf{3}$ were determined as a function of both $s\text{pH}$ and added $[\text{La}(\text{OTf})_3]$ with the original data being given in Tables S1–S20 (Supporting Information). As we have observed previously in the case of nonbinding substrates such as activated amides, esters, and paraoxon,^{13,14a,b,e} the concentration plots exhibit two domains attributable to the speciation of La^{3+} . At low but increasing concentration of La^{3+} (up to $\sim 2.5 \times 10^{-4}$ M) there is a transition between monomeric and dimeric La^{3+} -containing species, while, above this concentration, the plots become linear suggesting that all the material is in the form of active dimers. Following the approach we used before,^{14a,b,e} the slope of the linear portion of these plots was used to calculate the observed second-order rate constants (k_2^{obs}) for La^{3+}_2 -catalyzed methanolysis of $\mathbf{2}$ and $\mathbf{3}$ at the various $s\text{pH}$ values. These are listed in Tables 1 and 2 and are graphically presented in Figure 1 as $\log k_2^{\text{obs}}$ vs $s\text{pH}$ plots which seemingly plateau above $\sim s\text{pH}$ 8. Lines through the data are computed on the basis of fits to eq 5 involving the contributions of up to 3 species; vide infra.

In the case of La^{3+} -catalyzed methanolysis of nitrocefin the behavior of the concentration plots is different with typical plots of the k_{obs} vs $[\text{La}^{3+}]_{\text{total}}$ at three $s\text{pH}$ values being given in Figure 2 (for original data see Tables S21–S28 of the Supporting Information). The lines in Figure 2 are from fits to a model where sequential binding of 2 La^{3+}

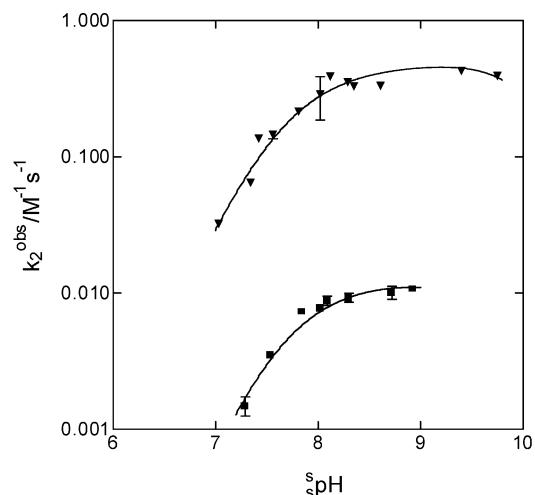


Figure 1. Plots of the k_2^{obs} vs s_{pH} for the La³⁺-catalyzed methanolysis of β -lactams **2** (■) and **3** (▼) at 25 °C under buffered conditions. Lines through the data are computed on the basis of fits to eq 5 containing up to three La³⁺₂(⁻OCH₃)_{*n*} species; vide infra.

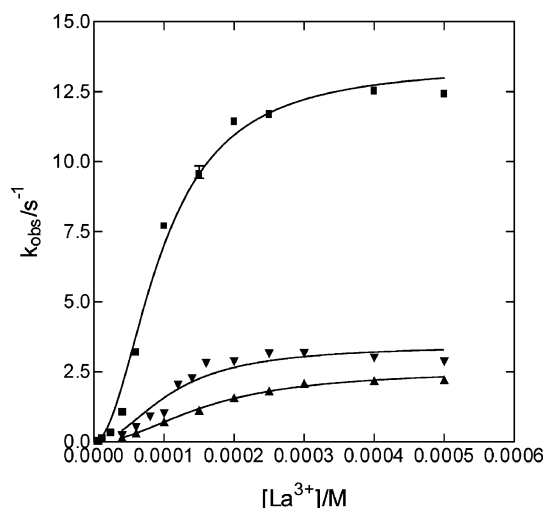


Figure 2. Plots of the k_{obs} vs $[\text{La}^{3+}]_{\text{total}}$ for catalyzed methanolysis of nitrocefins (**1**), $T = 25$ °C and s_{pH} 9.80 (■), s_{pH} 9.30 (▼), and s_{pH} 8.60 (▲).

ions to the substrate occurs which we have presented previously.^{14c} Because that fitting approach gives parameters that are heavily correlated, the best-fit values cannot be used in the absence of additional information, so we chose to base our kinetic analyses on a more detailed speciation description that is presented later. Each plot exhibits three general domains from low to high $[\text{La}^{3+}]_i$: linear at low concentrations, followed by a sigmoidal upturn at intermediate concentrations, followed by a plateau at high concentrations suggestive of saturation binding. The values of the constants at the plateau, $k_{\text{max}}^{\text{obs}}$, which represents the maximum observed pseudo-first-order rate constant for methanolysis of the La³⁺-bound nitrocefins, are plotted as a function of s_{pH} in Figure 3 with the original values being given in Table S29 in the Supporting Information. The two lines through the data are calculated as linear regressions of all points (slope 0.84 ± 0.05) and all points but the two highest s_{pH} (slope 1.02 ± 0.03), the meaning of which will be discussed later.

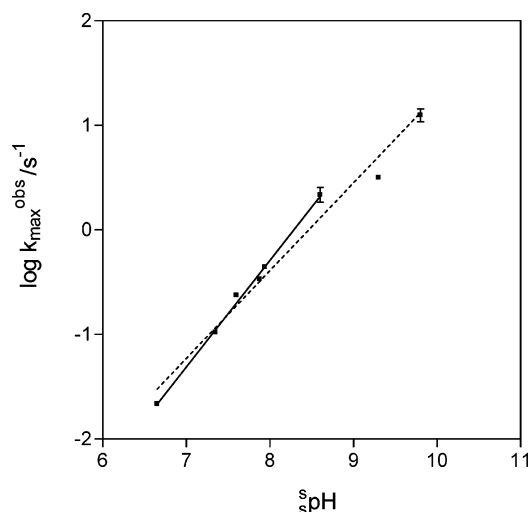
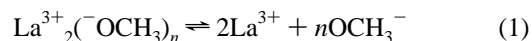


Figure 3. Plot of $\log k_{\text{max}}^{\text{obs}}$ for the La³⁺-catalyzed methanolysis of nitrocefins (**1**) as a function of s_{pH} , $T = 25$ °C. Lines through the data are linear regressions for all points (dotted line), slope = 0.84 ± 0.05 , and for the first 6 points (solid line), slope = 1.02 ± 0.03 .

(b) La³⁺ Speciation in Methanol. Recently we presented a study of the potentiometric titration of nine lanthanide metal ions as well as Zn²⁺, Cu²⁺, Co²⁺, Ni²⁺, and Ti⁴⁺ in methanol.¹⁹ Titration data for La³⁺ were obtained between $1 \times 10^{-3} \text{ M} \leq [\text{La}(\text{OTf})_3] \leq 3 \times 10^{-3} \text{ M}$, which is within the concentration range where the kinetic plots of k_{obs} vs $[\text{La}^{3+}]$ are linear for β -lactams **2** and **3**. The linear dependence of these plots gives no evidence of strong equilibrium binding to the metal ion. The potentiometric titration data were analyzed with the computer program Hyperquad¹⁸ through fits to the dimer model presented in eq 1 where n assumes values of 1–5, to give the various stability constants (sK_n) that are defined in eq 2.¹⁹ From the five computed stability constants, $\log sK_{1-5} = 11.66 \pm 0.04, 20.86 \pm 0.07, 27.52 \pm 0.09, 34.56 \pm 0.20,$ and 39.32 ± 0.26 , respectively, we determined the distribution of the various La³⁺₂(⁻OCH₃)_{*n*} forms as a function of s_{pH} at $[\text{La}(\text{OTf})_3]_{\text{total}} = 2 \times 10^{-3} \text{ M}$ (a full speciation diagram is shown as Figure 3 in ref 14e).



$$sK_n = [\text{La}^{3+}_2(\text{OCH}_3)_n] / [\text{La}^{3+}]^2 [\text{OCH}_3^-]^n \quad (2)$$

The methanolyses of the metal-bound forms of nitrocefins (**1**) were too fast to allow any titrations to determine the stoichiometry of the various species as a function of s_{pH} . Therefore, we resorted to using a nonreactive acid with the same general $s_{\text{p}}K_a$ as **1** (3,5-dinitrobenzoic acid, $s_{\text{p}}K_a$ in methanol 7.16 ± 0.01 , this work, vs kinetic $s_{\text{p}}K_a$ in methanol for **1** of 7.34^{12}). The formation constant for the species La³⁺₂(3,5-dinitrobenzoate⁻), as a model for the species La³⁺₂(1⁻), was calculated¹⁸ from the potentiometric titration of a solution of 0.02 M La(OTf)₃ and 0.01 M 3,5-dinitrobenzoic acid using the first 0.5 equiv of consumption of methoxide, corresponding to deprotonation of the La³⁺-bound carboxylic acid and comparing that apparent $s_{\text{p}}K_a$ with the $s_{\text{p}}K_a$ of the acid obtained from titration in the absence of metal ion. These concentrations are also well

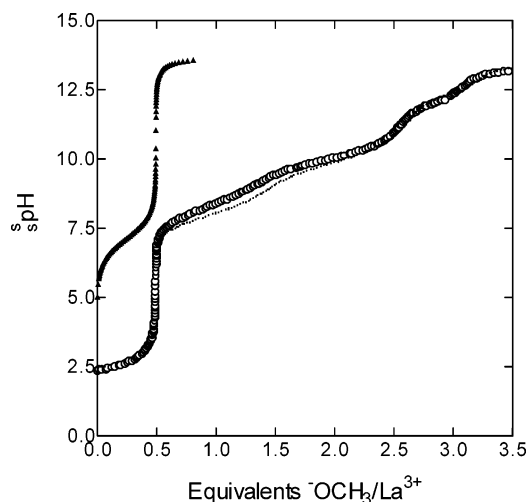
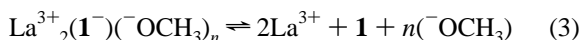


Figure 4. Potentiometric titration profiles for 0.02 M La(OTf)₃ (■), 0.01 M 3,5-dinitrobenzoic acid (▲), and a mixture of 0.02 M La(OTf)₃ and 0.01 M 3,5-dinitrobenzoic acid (○) determined in methanol at 25 °C.

above the saturation concentrations where the nitrocefin is completely bound to two La³⁺ ions in the plateau portions of the kinetic plots shown in Figure 2. Shown in Figure 4 are the titration curves used for the analysis. The ${}^sK_{1-5}$ formation constants pertaining to the La³⁺₂(⁻OCH₃)_{*n*} dimers obtained from the analysis of the titration of La(OTf)₃ by way of eqs 1 and 2 were input as constants for the computer analysis. The sK_n1 formation constants for the La³⁺₂(⁻OCH₃)_{*n*} species, defined analogously as in eqs 3 and 4, were assumed to be reasonably approximated by values obtained from the above titration of 2:1 La(OTf)₃–3,5-dinitrobenzoic acid using all but the first 0.5 equiv. Given in Table 3 are the so-derived constants.



$${}^sK_{0-5}1 = [\text{La}^{3+}_2(\mathbf{1}^-)(\text{}^-\text{OCH}_3)_n] / [\text{La}^{3+}]^2[\mathbf{1}^-][\text{}^-\text{OCH}_3]^n \quad (4)$$

(c) Fitting of the Kinetic Data. For lactams **2** and **3** the observed second-order rate constants (k_2^{obs}) were fitted as a function of ${}^s\text{pH}$ to the expression in eq 5, which is a linear combination of the contributions of the ${}^s\text{pH}$ -dependent species La³⁺₂(⁻OCH₃)₁, La³⁺₂(⁻OCH₃)₂, and La³⁺₂(⁻OCH₃)₃ at each ${}^s\text{pH}$ and where $k_2^{2:1}$, $k_2^{2:2}$, and $k_2^{2:3}$ are the second-order rate constants for the methanolysis of **2** or **3** promoted by the various dimeric forms.

$$k_2^{\text{obs}} = (k_2^{2:1}[\text{La}^{3+}_2(\text{}^-\text{OCH}_3)_1] + k_2^{2:2}[\text{La}^{3+}_2(\text{}^-\text{OCH}_3)_2] + k_2^{2:3}[\text{La}^{3+}_2(\text{}^-\text{OCH}_3)_3]) / [\text{La}(\text{OTf})_3]_t \quad (5)$$

The concentrations of the La³⁺₂(⁻OCH₃)_{*n*} forms at each ${}^s\text{pH}$ were calculated by HySS, a component of the Hyperquad suite of programs, using the formation constants previously determined.¹⁹ The values for the computed rate constants are given in Table 4. Shown in Figure 5 is a plot of the observed second-order rate constants for the catalyzed methanolysis of **3** as well as the contributions of various species as function of ${}^s\text{pH}$. From these it is clear that the dominantly active form is La³⁺₂(⁻OCH₃)₂. The data from

Table 3. log ${}^sK_{0-5}1$ and log ${}^sK_{1-5}$ Formation Constants for the La³⁺₂ Species Relevant to Kinetic Studies^a

La ³⁺ ₂ (⁻ OCH ₃) _{<i>n</i>} species	log ${}^sK_{0-5}1$
La ³⁺ ₂ (⁻ OCH ₃) ₀	9.8 ± 0.1 ^b
La ³⁺ ₂ (⁻ OCH ₃) ₁	18.14 ± 0.41 ^c
La ³⁺ ₂ (⁻ OCH ₃) ₂	26.39 ± 0.11 ^c
La ³⁺ ₂ (⁻ OCH ₃) ₃	32.62 ± 0.23 ^c
La ³⁺ ₂ (⁻ OCH ₃) ₄	39.78 ± 0.06 ^c
La ³⁺ ₂ (⁻ OCH ₃) ₅	44.38 ± 0.10 ^c
La ³⁺ ₂ (⁻ OCH ₃) _{<i>n</i>} species	log ${}^sK_{1-5}$
La ³⁺ ₂ (⁻ OCH ₃) ₁	11.67 ± 0.04 ^d
La ³⁺ ₂ (⁻ OCH ₃) ₂	20.94 ± 0.2 ^d
La ³⁺ ₂ (⁻ OCH ₃) ₃	27.61 ± 0.03 ^d
La ³⁺ ₂ (⁻ OCH ₃) ₄	34.68 ± 0.03 ^d
La ³⁺ ₂ (⁻ OCH ₃) ₅	39.55 ± 0.04 ^d

^a log K formation constant for La³⁺(⁻) from La³⁺ + ⁻ is 7.2 ± 0.1, assumed to be approximated by what is determined from Hyperquad analysis of titration data for a mixture of 1 × 10⁻² M in each of La(OTf)₃ and 3,5-dinitrobenzoic acid in methanol. ^b From the Hyperquad analysis of the first 0.5 equiv of ⁻OCH₃/La³⁺ of a titration of 0.02 M La(OTf)₃ in the presence of 0.01 M 3,5-dinitrobenzoic acid with the ${}^s\text{p}K_a$ of the latter set at 7.16. ^c From the Hyperquad analysis of all but the first 0.5 equiv of a titration of 0.02 M La(OTf)₃ in the presence of 0.01 M 3,5-dinitrobenzoic acid. ^d From the Hyperquad analysis of a titration of 0.002 M La(OTf)₃ with no added salts.¹⁹

Table 4. Computed Rate Constants for La³⁺₂(⁻OCH₃)_{*n*} Species in the Methanolysis of **2** and **3** Determined through Fits of k_2^{obs} at Each ${}^s\text{pH}$ to Eq 5^a

	La ³⁺ ₂ (⁻ OCH ₃) _{<i>n</i>} species	$k_2^{2:n}/\text{M}^{-1}\text{s}^{-1}$
2	La ³⁺ ₂ (⁻ OCH ₃) ₂	$k_2^{2:2} = 0.026 \pm 0.003$
	La ³⁺ ₂ (⁻ OCH ₃) ₁	$k_2^{2:1} = 0.06 \pm 0.01$
3	La ³⁺ ₂ (⁻ OCH ₃) ₂	$k_2^{2:2} = 0.98 \pm 0.11$
	La ³⁺ ₂ (⁻ OCH ₃) ₃	$k_2^{2:3} = 1.23 \pm 0.13$

^a Errors computed from the average % deviation in the fitted numbers calculated by eq 5 from the actual kinetic data.

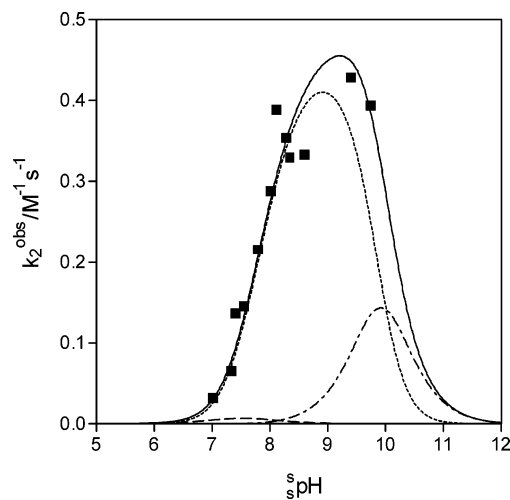


Figure 5. Plot of the contributions of various La³⁺₂(⁻OCH₃)_{*n*} forms to the k_2^{obs} for La³⁺-catalyzed methanolysis of **3** as a function of ${}^s\text{pH}$. Key: (—) combined effects of various species; (---) contribution of La³⁺₂(⁻OCH₃)₁; (···) contribution of La³⁺₂(⁻OCH₃)₂; (- · -) contribution of La³⁺₂(⁻OCH₃)₃; (■) actual k_2^{obs} kinetic data.

Table 4 can be used to calculate the solid line in the figure, which is a composite of the individual species contributions and passes through the observed kinetic values acceptably. A similar treatment (not shown) was performed for **2**, and its computed solid line is also given in the log/log plot of Figure 1.

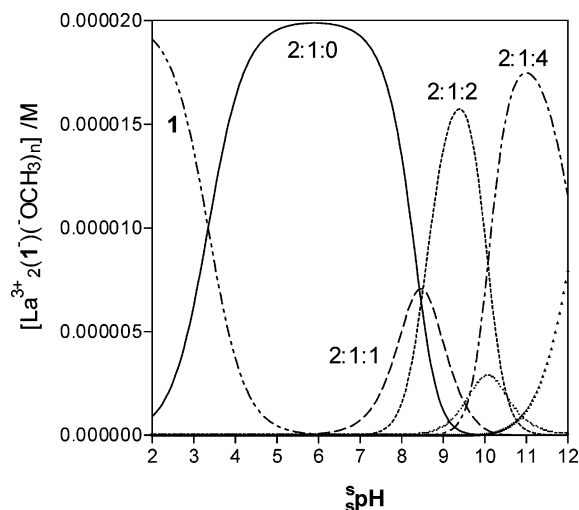


Figure 6. Speciation diagram for $\text{La}^{3+}_2(\mathbf{1}^-)(-\text{OCH}_3)_n$ forms as a function of $s\text{pH}$ computed from the formation constants given in Table 3 for titration of 2×10^{-5} M 3,5-dinitrobenzoic acid and 2×10^{-3} M La^{3+} . Values of 2:1:*n* refer to $\text{La}^{3+}_2(\mathbf{1}^-)(-\text{OCH}_3)_n$ forms with variable numbers of methoxides: (···) $\text{La}^{3+}_2(\mathbf{1}^-)(-\text{OCH}_3)_3$; (▲) $\text{La}^{3+}_2(\mathbf{1}^-)(-\text{OCH}_3)_5$.

Table 5. Computed $k'_{\text{max}}{}^{2:1:n}$ or $k_{\text{max}}{}^{2:1:n}$ Rate Constants for Various Species for the La^{3+} -Catalyzed Methanolysis of Nitrocefin (**1**) Computed from Fits of $k_{\text{max}}^{\text{obs}}$ vs $s\text{pH}$ Data to Eqs 7 and 6^a

model	$[\text{La}^{3+}_2(\mathbf{1}^-)(-\text{OCH}_3)_n]$	$k'_{\text{max}}{}^{2:1:n}$ or $k_{\text{max}}{}^{2:1:n}$
external methoxide model (eq 7)	$\text{La}^{3+}_2(\mathbf{1}^-)(-\text{OCH}_3)_0$	$k'_{\text{max}}{}^{2:1:0} = (2.9 \pm 0.4) \times 10^8{}^b$
	$\text{La}^{3+}_2(\mathbf{1}^-)(-\text{OCH}_3)_1$	$k'_{\text{max}}{}^{2:1:1} = (2.8 \pm 0.4) \times 10^8{}^b$
	$\text{La}^{3+}_2(\mathbf{1}^-)(-\text{OCH}_3)_2$	$k'_{\text{max}}{}^{2:1:2} = (0.66 \pm 0.09) \times 10^8{}^b$
internal methoxide model (eq 6)	$\text{La}^{3+}_2(\mathbf{1}^-)(-\text{OCH}_3)_1$	$k_{\text{max}}{}^{2:1:1} = 1.31 \pm 0.17{}^c$
	$\text{La}^{3+}_2(\mathbf{1}^-)(-\text{OCH}_3)_2$	$k_{\text{max}}{}^{2:1:2} = 1.62 \pm 0.22{}^c$
	$\text{La}^{3+}_2(\mathbf{1}^-)(-\text{OCH}_3)_3$	$k_{\text{max}}{}^{2:1:2} = 42.8 \pm 5.7{}^c$

^a Errors computed from the average % deviation in the fitted numbers calculated by eq 6 or 7 from the actual kinetic data. ^b $k'_{\text{max}}{}^{2:1:n}$ values are actually second-order rate constants in units of $\text{M}^{-1} \text{s}^{-1}$ after accounting for the $-\text{OCH}_3$ concentration. ^c $k_{\text{max}}{}^{2:1:n}$ values in units of s^{-1} .

In the case of **1** which is completely bound to La^{3+} dimers in the plateau portion of Figure 2, a similar approach was used, but because $\text{La}^{3+}_2(\mathbf{1})$ is too reactive to be determined by potentiometric titration, we required some nonreactive material as a model. The best-fit constants for the $\text{La}^{3+}_2(\mathbf{1}^-)(-\text{OCH}_3)_n$ species, assumed to be accurately approximated by the potentiometrically derived constants for the $\text{La}^{3+}_2(3,5\text{-dinitrobenzoate}^-)(-\text{OCH}_3)_n$ species, were used to determine their concentrations at each $s\text{pH}$. Shown in Figure 6 is the full speciation diagram computed under conditions where $[\mathbf{1}] = 2 \times 10^{-5}$ M and $[\text{La}^{3+}]_t = 2 \times 10^{-3}$ M.

These species were assumed to be the kinetically active ones that were used to fit the $k_{\text{max}}^{\text{obs}}$ plot shown in Figure 3. Two possible models for the kinetic behavior were considered involving (i) internal La^{3+}_2 -bound $-\text{OCH}_3$ acting as the nucleophile on coordinated **1** and (ii) external attack of methoxide on each $\text{La}^{3+}_2(\mathbf{1}^-)(-\text{OCH}_3)_n$ species. For the first model involving only $\text{La}^{3+}_2(\mathbf{1}^-)(-\text{OCH}_3)_n$ delivering an internally coordinated methoxide, a linear combination of active species described by the expression given in eq 6 was used, where $k_{\text{max}}{}^{2:1:n}$ are the best-fit pseudo-first-order rate constants for each bound La^{3+} dimer with “*n*” methoxides. In the second analysis, where external methoxide is the active nucleophile on any of the La^{3+}_2 -bound forms, the expression given in eq 7 was used to fit the $k_{\text{max}}^{\text{obs}}$ data. The best-fit

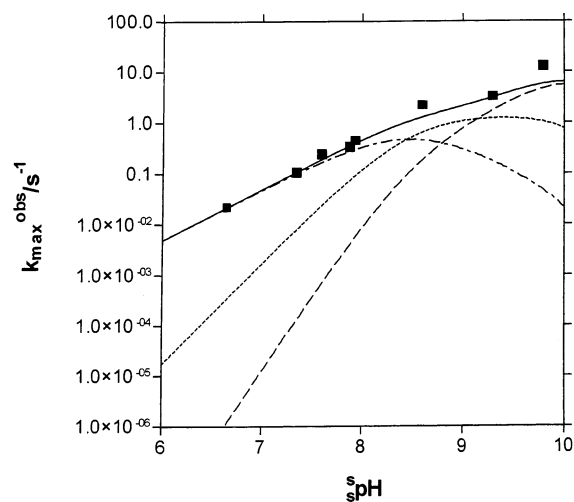


Figure 7. Plot of the $k_{\text{max}}^{\text{obs}}$ vs $s\text{pH}$ for the La^{3+}_2 -catalyzed methanolysis of **1**. Lines come from the fit of the kinetic data to eq 6: (—) composite of all contributions; (- · -) contribution of $\text{La}^{3+}_2(\mathbf{1}^-)(-\text{OCH}_3)_1$; (···) contribution of $\text{La}^{3+}_2(\mathbf{1}^-)(-\text{OCH}_3)_2$; (- - -) contribution of $\text{La}^{3+}_2(\mathbf{1}^-)(-\text{OCH}_3)_3$.

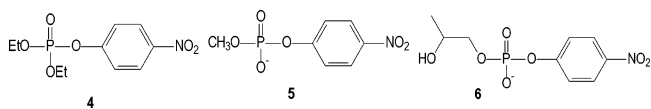
values for the various constants from each model are given in Table 5. Shown in Figure 7 is a plot of the $k_{\text{max}}^{\text{obs}}$ vs $s\text{pH}$ data along with the fit given by eq 6. The fit to eq 7 is mathematically identical to the fit to eq 6 because the two mechanisms these describe are kinetically indistinguishable. The derived constants have different meanings and are therefore not included in the figure but will be discussed later.

$$k_{\text{max}}^{\text{obs}} = \sum_{n=1}^3 k_{\text{max}}{}^{2:1:n} [\text{La}^{3+}_2(\mathbf{1}^-)(-\text{OCH}_3)_n] / [\mathbf{1}]_{\text{total}} \quad (6)$$

$$k_{\text{max}}^{\text{obs}} = \sum_{n=0}^2 k'_{\text{max}}{}^{2:1:n} [\text{La}^{3+}_2(\mathbf{1}^-)(-\text{OCH}_3)_n] [-\text{OCH}_3] / [\mathbf{1}]_{\text{total}} \quad (7)$$

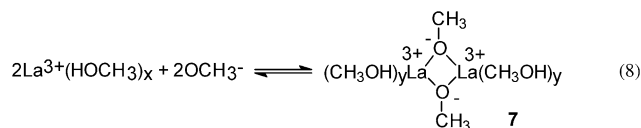
Discussion

All the La^{3+} -catalyzed methanolysis reactions that we have investigated fall broadly into two categories, namely those where there is no kinetically observed binding of the substrate to any of the La^{3+} forms and those where there is strong binding. The former category includes uncharged esters,^{14b} activated amides such as acetyl imidazole,^{14a} and phosphate triesters such as paraoxon (**4**),^{14e} while the latter category includes anionic substrates such as the phosphate diesters methyl-*p*-nitrophenyl phosphate (**5**)^{14c} and 2-hydroxypropyl *p*-nitrophenyl phosphate (**6**).^{14d} In the former category, where there is no strong binding of the substrate to the metal, above a relatively low $[\text{La}^{3+}]$ of 2.5×10^{-4} M the kinetics become linear in metal ion concentration because of the complete formation of La^{3+} dimers. At these concentrations, the kinetics exhibit good second-order behavior, first order in each of substrate and La^{3+} dimer. Such is the case with the simple lactams **2** and **3** studied here.



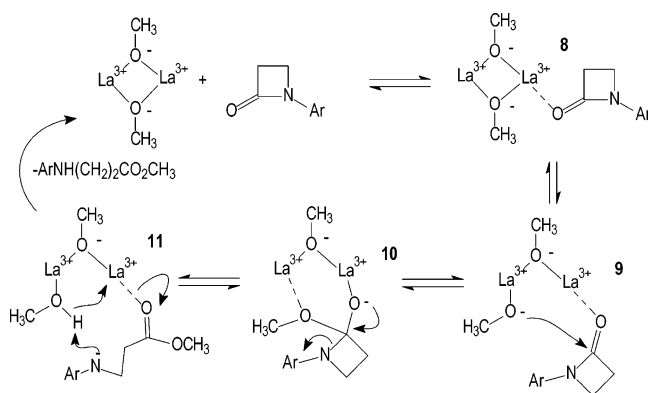
On the other hand, when there is strong binding of the metal ion(s) to the substrate, the kinetics at a given $s\text{pH}$ generally exhibit domains where first one La^{3+} binds to the substrate and, with further increases in $[\text{La}^{3+}]$, a second metal ion binds to the substrate. Both of the La^{3+} - and La^{3+}_2 -bound forms exhibit catalysis that has some dependence on $s\text{pH}$ as is the case in this study with nitrocefin. Where comparison can be made with binding of substrates to La^{3+} in water, binding in methanol is markedly stronger due to the reduced dielectric constant of the medium relative to water (31.5 vs 78.5 at 25 °C).²⁰ For example, in the case of 2-hydroxypropyl *p*-nitrophenyl phosphate (**6**), the binding constant with one La^{3+} in water is 74 M^{-1} ,²¹ while in methanol it is at least 10^4 -fold stronger at $>10^6 \text{ M}^{-1}$.^{14d} Moreover, in water there is little propensity for binding more than one metal ion unless chelating ligands are present to predispose formation of dinuclear complexes. In methanol La^{3+} , at concentrations $>2 \times 10^{-4} \text{ M}$, spontaneously forms very active dimeric species which, in the case of $\text{La}^{3+}_2(\text{OCH}_3)_2$, we have formulated as a doubly bridged dimer (**7** in eq 8).

Other forms with the stoichiometry $\text{La}^{3+}_2(\text{OCH}_3)_{1,3,4,5}$ can be identified from potentiometric titration¹⁹ and, in selected cases, by electrospray mass spectrometry.^{14b} Some of these, for example with 1 and 3 methoxides, have been shown to have activity for methanolysis reactions of *p*-nitrophenyl acetate^{14b} and paraoxon.^{14c}



(a) La^{3+} -Catalyzed Methanolysis of Simple Lactams **2 and **3**.** On cursory inspection, the appearance of the $\log k_2^{\text{obs}}$ vs $s\text{pH}$ plots for the methanolysis of **2** and **3** shown in Figure 1 suggests the plateau results from formation of an active species generated by ionization of a single group associated with the catalyst which has an apparent $s\text{pK}_a$ of $\sim 7.5\text{--}7.8$. If we follow that line of reasoning, the maximal second-order rate constant for catalysis of the methanolysis of **2** and **3** at the plateau would be 1×10^{-2} and $35 \times 10^{-2} \text{ M}^{-1} \text{ s}^{-1}$, respectively. The 35-fold difference is attributed to the electron-withdrawing effect of the NO_2 group increasing the electrophilicity of the $\text{C}=\text{O}$ unit of **3**.

A deeper analysis of the kinetics must take due cognizance of the La^{3+} speciation as a function of $s\text{pH}$ since this changes throughout the $s\text{pH}$ region where the kinetics are determined. The speciation is available through computer fitting of the La^{3+} potentiometric titration data obtained at concentrations of 1 to $3 \times 10^{-3} \text{ M}$ (where the kinetics are linear in $[\text{La}^{3+}]_t$) to the model given in eqs 1 and 2.¹⁹ Up to $s\text{pH} \sim 9.7$, the highest $s\text{pH}$ where the kinetics were determined, the dominant forms are $\text{La}^{3+}_2(\text{OCH}_3)_n$, $n = 1\text{--}3$.

Scheme 1^a

^a Methanols of solvation were omitted for clarity.

The most abundant species is $\text{La}^{3+}_2(\text{OCH}_3)_2$ between $s\text{pH}$ 8 and 10 (maximum concentration of $\sim 80\%$ of the total La^{3+} -containing species at $s\text{pH}$ 8.9), but $\text{La}^{3+}_2(\text{OCH}_3)_1$ and $\text{La}^{3+}_2(\text{OCH}_3)_3$ are also present to a lesser extent (maximum concentrations of $\sim 25\%$ of the total La^{3+} -containing species in each reached at respective $s\text{pH}$ values of 7.5 and 10).

To assess the catalytic viability of these forms, we fit the k_2^{obs} values to a linear combination of the contributions of the various forms (eq 5) and determined that $\text{La}^{3+}_2(\text{OCH}_3)_2$ and $\text{La}^{3+}_2(\text{OCH}_3)_3$ contribute prominently and $\text{La}^{3+}_2(\text{OCH}_3)_1$ far less so to the overall kinetics for methanolysis of **3** while only $\text{La}^{3+}_2(\text{OCH}_3)_2$ is required to explain the methanolysis of **2** up to $s\text{pH}$ 8.92. The best-fit values for all the constants are given in Table 4. As can be judged by the plot shown in Figure 5 for methanolysis of **3**, and by the calculated lines through the kinetic data for **2** and **3** in Figure 1, the fittings account for the observed kinetic data very well.

In either case the species that contributes most of the activity in the $s\text{pH}$ range investigated is $\text{La}^{3+}_2(\text{OCH}_3)_2$ with computed second-order rate constants of 0.026 and $0.98 \text{ M}^{-1} \text{ s}^{-1}$ for the methanolysis of **2** and **3**, respectively. In the case of **3** the rate constant for the $\text{La}^{3+}_2(\text{OCH}_3)_3$ species is larger at $1.23 \text{ M}^{-1} \text{ s}^{-1}$, but overall that species does not contribute so much to the kinetics because its concentration is lower than that of $\text{La}^{3+}_2(\text{OCH}_3)_2$. These constants can be compared with the second-order rate constants for the methoxide reactions, 0.0026 and $0.43 \text{ M}^{-1} \text{ s}^{-1}$ respectively for **2** and **3**.^{22,23} The overall catalytic effect of the composite reactions catalyzed by all the species can be judged in comparison to the base-catalyzed reaction at a neutral $s\text{pH}$ of 8.4, where the $[\text{OCH}_3^-]$ is $4.27 \times 10^{-9} \text{ M}$ and a 1 mM solution of catalyst (generated from 2 mM of $\text{La}(\text{OTf})_3$) accelerates the methanolysis of **2** by $\sim 2 \times 10^7$ -fold and **3** by $\sim 5 \times 10^5$ -fold. Interestingly, there is a 40-fold larger catalytic effect for the less reactive lactam.

In Scheme 1 is a proposed mechanism for $\text{La}^{3+}_2(\text{OCH}_3)_2$ -catalyzed methanolysis of the simple β -lactams. Neither **2** nor **3** binds strongly to any form of La^{3+} since, under the conditions investigated, the kinetics are strictly second-order

(20) Harned, H. S.; Owen, B. B. *The Physical Chemistry of Electrolytic Solutions*, 3rd ed.; ACS Monograph Series 137; Reinhold Publishing: New York, 1957; p 161.

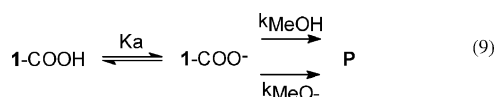
(21) Morrow, J. R.; Buttrely, L. A.; Berback, K. A. *Inorg. Chem.* **1992**, *31*, 16.

(22) Broxton, T. J.; Deady, L. W. *J. Org. Chem.* **1974**, *39*, 2767.

(23) By way of comparison, the HO^- reaction in water has reported second-order rate constants of 1.3×10^{-3} and $50 \times 10^{-3} \text{ M}^{-1} \text{ s}^{-1}$, respectively.^{15b}

overall with no evidence of any saturation phenomenon. Nevertheless it is difficult to envision any catalytic process without some transient substrate–catalyst complex being formed (**8** in Scheme 1). This is because the computed second-order rate constants for the active La³⁺₂(-OCH₃)₂ form are similar to or slightly larger than those for methoxide even though the ^spK_a for the metal-bound HOCH₃ is reduced from that of unbound methanol by roughly 9 units. Consequently, a metal-stabilized methoxide should be substantially less nucleophilic than free methoxide by virtue of a normal Brønsted relationship unless an additional role for the metal is operative such as acting as a Lewis acid to activate the C=O. A methoxy group bridged between two La³⁺ ions, as in **4**, may not be sufficiently nucleophilic^{24,25} to attack the coordinated lactam so, as we have previously proposed for the analogous reactions with the far less reactive phosphate triester paraxon,^{14e} it is possible that one of the La³⁺-OCH₃-La³⁺ bridges opens to reveal a singly coordinated La³⁺-OCH₃ (**9**). This then undergoes intramolecular nucleophilic addition to the C=O (**10**) followed by ejection of the N leaving group to give **11** from which the active La³⁺₂(-OCH₃)₂ form is regenerated. Whether departure of the anionic N occurs with coordination to the metal ion or how it becomes protonated cannot be assessed at this time.

(b) La³⁺-Catalyzed Methanolysis of **1.** The ^spH vs log *k*_{obs} profile for the methanolysis of **1** in the absence of metal ions¹² consists of three domains and was analyzed in terms of the mechanism presented in eq 9. The ascending portion at low ^spH with a kinetic ^spK_a of 7.34 for the COOH gives rise to a plateau from ^spH 7.5–12 (*k*_{MeOH} = 8.96 × 10⁻⁵ s⁻¹) for methanol attack, probably with general base assistance by the internal COO⁻, followed by a CH₃O⁻ domain having *k*_{MeO} = 1.18 M⁻¹ s⁻¹.



The plots of *k*_{obs} vs [La³⁺]_t shown in Figure 2 for methanolysis of **1** show, at low [La³⁺], evidence of very strong 1:1 binding, which gives way to saturation 2:1 binding on further increases in [La³⁺]. Analysis of the potentiometric titration data for a mixture containing 2 × 10⁻³ M in each of La(OTf)₃ and 3,5-dinitrobenzoic acid gives a log formation constant for La³⁺ + ArCOO⁻ ⇌ La³⁺-O₂CAr of 10^(7.2±0.1) M⁻¹, which we take as a reasonable approximation for the formation constant of La³⁺(1⁻). The binding constant for the process La³⁺ + La³⁺(1⁻) ⇌ La³⁺₂(1⁻) can then be computed as 10^{2.6} M⁻¹ from the log ^sK₀¹ data in Table 3 for the

species La³⁺₂(1⁻)(-OCH₃)₀. This constant indicates that metal saturation should be observed at millimolar concentrations, nicely verifying the situation shown in Figure 2. It is important to realize, on the basis of the first and second binding constants, that above a concentration of ~10⁻⁶ M in La³⁺, when in excess of [**1**], at least one metal ion is bound, and above 10⁻³ M, the second La³⁺ is bound. The data in Table 3 can also be used to compute the binding constants of 1⁻ to any of the La³⁺₂(-OCH₃)_n forms simply as (log ^sK_n¹ - log ^sK_n). Interestingly, these binding constants range from 10^{6.47} to 10^{4.83} M⁻¹ as one sequentially adds methoxide. In the order from La³⁺₂(1⁻)(-OCH₃) to La³⁺₂(1⁻)(-OCH₃)₅, the progressively lower affinity of the 1⁻ for the species with larger number of methoxides is probably due to the reduced overall positive charge on the bound species.

What concerns us here is the overall speciation of bound forms of 1⁻ (La³⁺₂(1⁻)(-OCH₃)_n) as a function of ^spH at high concentrations of La³⁺ corresponding to those in the plateau portion of the *k*_{obs} vs [La³⁺] plots (see Figure 2). The La³⁺₂(1⁻)(-OCH₃)_n speciation diagram shown in Figure 6 reflects the kinetic conditions of 2 × 10⁻⁵ M **1** and 2 × 10⁻³ M [La³⁺]_{total}. Inspection of the diagram indicates that between ^spH 6 and 10, where the kinetics of methanolysis of La³⁺₂-bound 1⁻ were monitored, the major species are La³⁺₂(1⁻)(-OCH₃)₀, La³⁺₂(1⁻)(-OCH₃)₁, La³⁺₂(1⁻)(-OCH₃)₂, La³⁺₂(1⁻)(-OCH₃)₃, and La³⁺₂(1⁻)(-OCH₃)₄. The involvement of the latter species and also La³⁺₂(1⁻)(-OCH₃)₅, which appears at higher ^spH, cannot be ascertained from fits to the kinetic data and are therefore not included as relevant reactants. The diagram also illustrates that **1** is completely bound by ^spH 5.

There are two kinetically indistinguishable mechanisms that can be considered for fitting the kinetic data for methanolysis of the La³⁺₂(1⁻)(-OCH₃)_n species. The first mechanism, described by eq 6, involves spontaneous methanolysis of the of La³⁺₂(1⁻)(-OCH₃)_n forms, the amounts of which vary with ^spH in a way predicted by their formation constants. The fit to the kinetic data shown in Figure 7 indicates that the pseudo-first-order rate constants (see Table 5) for the La³⁺₂(1⁻)(-OCH₃)_n forms responsible for spontaneous methanolysis increase with numbers of added methoxides. The contributions of each form to the fit shown in Figure 7 can then be determined on the basis of how much of each is present at any ^spH, coupled with its rate constant for reaction. The fit is remarkably good given the inherent assumptions that the 3,5-dinitrobenzoate complexes accurately represent the speciation for the nitrocefin complexes.

The second mechanism involves an attack of external methoxide on La³⁺₂(1⁻)(-OCH₃)_n, but because this is kinetically equivalent to the internal methoxide mechanism, the form susceptible to methoxide attack at any given ^spH must have one less bound methoxide than the form responsible for the internal or spontaneous methanolysis process described above. Overall the fit obtained with eq 7 is identical to that obtained with eq 6, but the rate constants (Table 5) are now second-order ones with values of 2.9 × 10⁸, 2.8 ×

(24) (a) Williams, N. H.; Cheung, W.; Chin, J. *J. Am. Chem. Soc.* **1998**, *120*, 8079. (b) Wahnon, D. Lebuis, A.-M.; Chin, J. *Angew. Chem., Int. Ed. Engl.* **1995**, *34*, 2412.

(25) Recent studies with dinuclear Zn²⁺ enzymes and theoretical analyses of such have also considered an opening of the μ-hydroxo bridge prior to nucleophilic attack on bound substrate.^{6a} Bennett, B.; Holz, R. C. *J. Am. Chem. Soc.* **1997**, *119*, 9, 1923. Zhan, C. G.; deSouza, O. N.; Rittenhouse, R.; Ornstein, R. L. *J. Am. Chem. Soc.* **1999**, *121*, 7279. Suárez, D.; Brothers, E. N.; Merz, K. M., Jr. *Biochemistry* **2002**, *41*, 6615. Díaz, N.; Suárez, D.; Merz, K. M., Jr. *J. Am. Chem. Soc.* **2000**, *120*, 4197. Krauss, M.; Gilson, H. R. S.; Gresh, N. *J. Phys. Chem. B* **2001**, *105*, 8040.

10^8 , and $0.66 \times 10^8 \text{ M}^{-1} \text{ s}^{-1}$ for methoxide attack on $\text{La}^{3+}_2(\mathbf{1}^-)(\text{OCH}_3)_0$, $\text{La}^{3+}_2(\mathbf{1}^-)(\text{OCH}_3)_1$, and $\text{La}^{3+}_2(\mathbf{1}^-)(\text{OCH}_3)_2$, respectively.

There is nothing by way of argument that might allow one to prefer one or the other mechanism. The computed second-order rate constants for methoxide on the bound forms are high at $\sim 10^8 \text{ M}^{-1} \text{ s}^{-1}$ but are well below the limit of $\sim 10^{10} \text{ M}^{-1} \text{ s}^{-1}$ which would be appropriate for a diffusion-limited process involving reaction of an anion and a positively charged species.²⁶ These values compare favorably with the rate constant for attack of CH_3O^- on the $(\text{NH}_3)_5\text{-Co}^{\text{III}}$ complex of acetylimidazole, another activated amide positively charged by virtue of metal coordination, for which a k_2 of $4.69 \times 10^7 \text{ M}^{-1} \text{ s}^{-1}$ was determined.^{14a,27} Relative to the uncatalyzed attack of CH_3O^- on $\mathbf{1}^-$ ($k_{\text{OMe}} = 1.18 \text{ M}^{-1} \text{ s}^{-1}$) putative attack of methoxide on the $\text{La}^{3+}_2(\mathbf{1}^-)(\text{OCH}_3)_{0,1,2}$ forms is accelerated by some 10^8 -fold. Regardless of which mechanism is actually operative, a comparison can be made for the La^{3+} -promoted methanolysis of fully bound $\mathbf{1}$ at neutral s_pH of ~ 8.4 ($k_{\text{max}}^{\text{obs}} = \sim 1 \text{ s}^{-1}$) with the spontaneous methanolysis of $\mathbf{1}^-$ ($k_{\text{MeOH}} = 8.96 \times 10^{-5} \text{ s}^{-1}$)¹² for an observed acceleration of $\sim 10^4$ -fold.

Conclusions

In the above we have shown that La^{3+} dimers markedly accelerate the methanolysis of two simple *N*-aryl- β -lactams which do not have metal binding sites and nitrocefin in which there is strong equilibrium La^{3+}_2 -binding to the COO^- . Two main points are revealed by the in-depth study of the La^{3+}_2 speciation as pertains to the two types of β -lactams. Where there is no strong binding (e.g. with $\mathbf{2}$ and $\mathbf{3}$), the catalytically active forms are $\text{La}^{3+}_2(\text{OCH}_3)_n$ in which the numbers of associated methoxides vary from 1 to 3 as a function of s_pH with the dominant catalytic species having 2 methoxides. This form was earlier shown to be catalytically active for methanolysis of carboxylate esters, both nonactivated and activated,^{14b} the activated amide acetyl imidazole,^{14a,27} and paraoxon.^{14c} While none of these exhibits strong equilibrium binding, it is difficult to envision a satisfactory mechanism

without transient binding to the La^{3+} dimers prior to the actual methanolysis reaction. The role of the catalyst is then to provide both Lewis activation and delivery of a La^{3+} -bound methoxide.

This type of catalytic activity was not previously observed for Zn^{2+} in solution with simple lactams that do not contain a pendant group such as COO^- that can bind to the metal ion thus enforcing its proximity with the scissile $(\text{N})\text{C}=\text{O}$ unit. The fact that the La^{3+} dimer does catalyze methanolysis of the simple lactams points to some special property or set of properties that could include ability to bind the $\text{C}=\text{O}$ unit by one of the metal ions as a Lewis acid to activate it toward nucleophilic attack by the methoxide associated with the second metal ion. These features may be related to the catalysis exhibited toward lactam hydrolysis in the active site of the dinuclear Zn^{2+} - β -lactamases.

When the substrate contains an anionic group such as COO^- or $(\text{ArO})_2\text{PO}_2^-$,^{14c} there is a strong equilibrium binding with one La^{3+} , but this does not, in the case of nitrocefin, give a complex which shows marked catalysis. Binding of a second La^{3+} yields a species that is far more active for the methanolysis process, and the reason for this may be that a bound dimeric form of La^{3+} may position the metal ions nearer to the reactive site to provide catalysis of the methanolysis. The activities of the $\text{La}^{3+}(\mathbf{1}^-)$ or $\text{La}^{3+}(\text{O}_2\text{P}(\text{OAr})_2)$ forms increase with s_pH in a way which may appear to be first order in $[\text{OCH}_3^-]$ or decidedly less than first order (0.5 order in the case of methyl *p*-nitrophenyl phosphate^{14c}). Understanding why this is so requires due consideration of the La^{2+} -bound species and how these change as a function of s_pH . In the case of nitrocefin, we have dissected the s_pH dependence of these species and shown that two kinetically equivalent mechanisms can account for the overall behavior.

Acknowledgment. The authors are indebted to the Natural Sciences and Engineering Research Council of Canada and Queen's University for financial support of this work. In addition, G.T.T.G. thanks the NSERC for the award of a PGS A graduate fellowship.

Supporting Information Available: Tables S1–S29 of kinetic data for k_{obs} vs $[\text{La}^{3+}]_t$ for the methanolysis of $\mathbf{1}$ – $\mathbf{3}$. This material is available free of charge via the Internet at <http://pubs.acs.org>.

IC0302736

(26) (a) Fersht, A. *Enzyme Structure and Mechanism*; W. H. Freeman and Co.: New York, 1985; pp 147–8. (b) Eigen, M.; De Maeyer, L. Z. *Electrochem.* **1955**, *59*, 986.

(27) Neverov, A. A.; Montoya-Pelaez, P.; Brown, R. S. *J. Am. Chem. Soc.* **2001**, *123*, 210.